

# Secondary Forest Mapping by Utilizing Sentinel-2 MSI Imagery

<sup>1</sup>Jwan Al-Doski\*, <sup>2</sup>Shattri B. Mansor, <sup>3</sup>Zailani Khuzaimah

<sup>1,2,3</sup> Department of Civil Engineering, Faculty of Engineering, Universiti Putra Malaysia 43400, Serdang, Selangor, Malaysia

Email: <sup>1</sup>Aldoski-Jwan@hotmail.com, <sup>2</sup>shattri@gmail.com, <sup>3</sup>zailanikhuzaimah@gmail.com

\* Corresponding author e-mail address: Aldoski-Jwan@hotmail.com

---

**Abstract:** The research region covered by the secondary forest and it has quickly extended. Estimating either beneficial economic or environmental impacts needs accurate maps. Sentinel-2 Multispectral Instrument (MSI) with its distinctive synoptic coverage capability provides accurate and instantly valuable data. Three classification techniques (Artificial Neural Network (ANN), Support Vector Machine (SVM) and Spectral Angle Mapper (SAM)) were investigated in this paper utilizing Sentinel-2 MSI image with training samples of various sizes to map secondary forest cover. SVM had the perfect output with overall accuracy varying from 86% to 92% and a coefficient of Kappa from 0.76 to 0.85, depends entirely on the sample size of the training data (varying from 20 to 500 pixels per class). SVM's benefit was more apparent once the sample size of the training was lower. ANN needed the involvement of the user, the level of his / her knowledge and experience affected the accuracy. The SAM algorithm surpassed alike SVM and ANN in aspects of speed and efficiency for large-scale secondary forest mapping. Furthermore, the maximum threshold values of the SAM spectral angle for a large training sample size are in agreement with the outcomes of previous studies, that implies the potential subjectivity of the SAM threshold. If verifiable, the SAM algorithm will be a simple and robust methodology commonly for large-scale mapping of secondary forest.

**Keywords:** Artificial Neural Network; Vector Machine Support; Spectral Angle Mapper; Sentinel-2 MSI.

---

## I. INTRODUCTION

Secondary forest mapping has been acknowledged as a fundamental task for science, environmental and policy data, forest management, statistics, and financial reasons, environmental issues, and sustainable forest management at the global, regional and local level. Environmental studies concerning biogeochemical cycles, natural resource conservation and management, urban planning, food and health, among others, and earth system researchers as entry into forest models. In addition, modifications in the secondary forest region induced by human and abiotic and biotic changes (1) Due to changing climate circumstances, data is important (1-3). Remote sensing with a wide range of spatial and spectral resolution is the most important technology for effective secondary forest cover mapping on a global, regional and local scale to define the spatial area and extent of the secondary forest, putting numerous benefits like cost-effectiveness and repeatable of observations. (4, 5). Satellite optical and radar imagery has been commonly used to classify, define and map secondary forest cover (6-8).

Several authors used various remotely sensed optical information and various algorithms to map the forest. For example, Shen et al. (9) investigated the Mapping possibility of forest ecosystems at tree-level species from elevated spatial resolution hyperspectral imagery (AISA) in Hachioji, Japan. Eight standard classification techniques were evaluated for mapping performance such as SAM, which obtained the highest outcome. Additionally, Kachmar et al. (10) applied Landsat 5 TM information for the classification of prevalent forest cover types in Japan's Naeba Mountains in the SAM classification. Though, using either certain spectral class thresholds or using spectral angle mapper classifiers, imaging techniques are problematic due to the quickly evolved canopy that allows secondary forest cover spectrally similar to

other types of land cover. (11-13) Saturation of the ideal images created by the closure of the canopy will also decrease forest viewing from other land cover classes (14). Regular cloud coverage in humid tropical areas prevents the acquisition of cloud-free optical satellite images to observe large secondary forest areas (15). By contrast, satellite radar imagery is all-weather and worthy of all-time. Many scientists thus use radar satellite information to track and map forests in tropical regions (8, 16). The comparatively excellent secondary forest mapping capabilities from both airborne and spatial radar sensors have been demonstrated by different authors (17-19). Radar systems are able to obtain usable information independently of daylight and atmospheric circumstances, unlike optical sensor systems. This is a separate benefit, especially for apps requiring timely data. The most prevalent weakness of both airborne and spatial radar detectors is their topography sensitivity. (20, 21). Topographic variations influence the radar backscatter's power and therefore generate tonal distinctions in radar images. Variations in image tone caused by topography can be readily confused with tonal variations arising from other influences (e.g. cover type transitions) and thus complicate radar image visual and/or computer assessment. Image analysis methods are being developed to compensate for topographical impacts (22, 23).

New possibilities open to Earth Observation with the creation of the latest European Space Agency Sentinel-1, -2, -3 satellite constellation. The series offers the scientific community with high operational capacity, long-term stability, superior sensor calibration and a range of sensing techniques and products (24). Also, the main benefit of a complete free and open access policy for most items is the distribution of Sentinel information. (25). On 23 June 2015, as part of the European Copernicus program, the Sentinel-2A satellite was effectively introduced and the first scenes were supplied a few days later (26). Sentinel-2 (S2) provides an innovative wide-ranging, high-resolution, multi-spectral imaging system (MSI) with 13 spectral bands, offering unbelievable land and vegetation views (26). It is supposed that the combination of increased resolution (up to 10 m), new spectral capabilities (e.g., three bands in the red-edge plus two bands in the SWIR), wide coverage (290 km swath width) and a minimum of five days of global revision time (with twin satellites in orbit) provides incredibly useful information for a wide range of land (and coastal) entries (25). In other terms, Sentinel-2A's distinctive mix of features reflects an unprecedented capacity for regional and global land cover descriptions and mapping (26). The scientific community has been seeking to provide feedback to system designers to determine the best algorithms and approaches for information exploitation in preparing for Sentinel's new satellite mission. This activity resulted in several studies reporting elevated ability of Sentinel information in different areas of implementation, however, actual information must be verified. Sentinel satellite information for science and commercial reasons are now accessible and willing to be used.

In recent years, various classification algorithms range from parametric to non-parametric techniques to secondary forest cover mapping (27). Parametric methods (e.g., maximum likelihood) that suppose information is normally distributed and involve a large number of calibration locations were regularly used to characterize the forest cover (28, 29) however, they are difficult since non-normal, multi-model and categorical information used in heterogeneous landscapes could be remotely sensed and ancillary. Non-parametric methods that do not presume a specific distribution of information have increased interest in studies over the last century (30). Classification Trees(31), Artificial Neural Network (ANN)(32), Spectral Angle Mapper (SAM)(33), Neural Networks (33)and Support Vector Machines (34, 35)are Among the most prevalent models powered by non-parametric used to map secondary forest cover. These non-parametric techniques, but, appear to over-fit the calibration information and are often hard to perform due to the test and error needed to determine user-defined model calibration parameter values(30, 36-38).

Nevertheless, the accuracy of the classification techniques varied depending on the classification techniques and the achievement of the discrimination often relies on the spectral difference between the secondary forest cover and other characteristics in the study region and needs unique expertise or skills to be used (39). By integrating various classification algorithms into operative instruments to use with Sentinel information, science attempts for secondary forest cover mapping are underway. To our understanding, furthermore, the combined use of SVM, ANN, and SAM as spectral-based classifiers with Sentinel-2 MSI imagery in the mapping of secondary forest cover areas has been restricted, if not exist, especially in tropical conditions. We are addressing this problem with the current research, so the goal is twofold: (1) to assess the ability of Sentinel-2 MSI imagery to map secondary forest and (2) to assess the efficacy of different classification techniques when using Sentinel-2 MSI information. We used SVM, ANN, and SAM techniques to map secondary forests in a tiny region in the state of Kelantan, randomly have chosen training samples of distinct sample sizes from a big set of training points to evaluate the efficiency of distinct classification techniques, intended to include Sentinel-2 MSI information with a viable selection algorithm reference for secondary forest mapping.

## II. MATERIAL AND METHOD

### 2.1 Study Area

The study area covering an area of approx. 553.6 km<sup>2</sup> in the Kuala Krai district of Kelantan State, Malaysia, situated among 102 ° 14'55.76"E and 102 ° 7'52.30"E and 5 ° 24'16.26"N and 5 ° 40'32.22"N among latitudes (Figure 1). The rainfall is a monthly mean rainfall of further than 6,000 mm. Approximately 27.5 C annual temperature. For secondary forest cover, the humid, equatorial environment is appropriate. It has been one of the region's main form of forest. In this way our study region is comparatively flat, the altitude of the test research rises gradually from 100-900 m above sea level.

### 2.2 Sentinel Data

Sentinel-2A is introduced in June 2015 and can be downloaded from (<https://scihub.copernicus.eu/>) to the public. Information from Sentinel-2A with Multispectral Instrument (MSI) is described by a range of 13 spectral bands with a ground spatial resolution varying from 10 m to 60 m (Table 1). Such spectral and spatial resolutions, together with the free accessibility of pictures, make Sentinel-2 very attractive for water mapping and flood tracking and other purposes such as forest and crop monitoring and mapping. (3, 40).

## III. METHODOLOGY

### 3.1 Data Per-processing

On 18 February 2016, Sentinel-2A MSI imagery was obtained at the geocoded level L1C (solar azimuth 127, solar elevation 66). The Sentinel-2A MSI-L1C datasets are Top of Atmosphere (TOA) reflectance's normal item and have been pre-processed. First, the atmospherically adjusted image utilizing sen2cor software version 2.3 (Telespazio VEGA Deutschland GmbH, Darmstadt, Germany) to create and format atmospheric bottom (BOA) Level-2A items using the Sen2Cor processor (version 2.3) under the platform of Anaconda Python. Sen2Cor allows the processing of Sentinel-2 L1C products for physical atmospheric, terrain and cirrus correction and produces corrected bands for BOA reflection (40). The format of the yield item is a compilation of TIFF images with three distinct resolutions (10, 20 and 60 m) replicated bands. In this research, we used 10 m resolution bands to obtain and classify secondary forests. The Sentinel-2 MSI picture was then geometrically corrected using 15 GCPs of significant characteristics (highways) and digital elevation models (DEM) to achieve enhanced geodesic precision and a geometrically corrected product free of inconsistencies (41, 42). The polynomial function of the first order was shown and a nearest-neighbor resampling protocol was implemented to correct systematic changes between neighboring pictures in a few instances. Total Root Mean Square Error (RMSE) transformation equivalent to 0.08 that was less than 1 pixel (43-45) and much less than the rigorous 0.5 pixel criteria (46, 47). The Sentinel-2 MSI image was then re-projected by using the closest neighborhood resampling technique to the Universal Transverse Mercator (UTM) coordinating scheme with datum WGS 1984 and zone 47 north. The data were spatially small subset to the study area see figure 2 (originally 20,490 or 15,489 pixels) with ENVI 5.1 software.

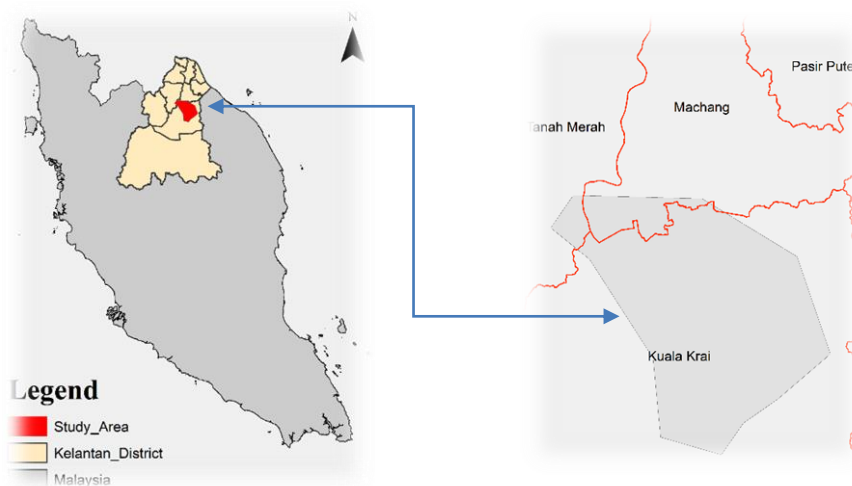


FIGURE 1. STUDY AREA LOCATION IN KELANTAN STATE, MALAYSIA

**TABLE 1. THE SENTINEL-2 MSI SENSOR SPECTRAL BAND DATA (IN THIS RESEARCH, BANDS 2, 3, 4, AND 8 WERE APPLIED).**

<i>Sentinel-2 Bands</i>	<i>Central Wavelength (<math>\mu\text{m}</math>)</i>	<i>Resolution (m)</i>	<i>Bandwidth (nm)</i>
<i>Band 1—Coastal aerosol</i>	0.443	60	20
<i>Band 2—Blue</i>	0.490	10	65
<i>Band 3—Green</i>	0.560	10	35
<i>Band 4—Red</i>	0.665	10	30
<i>Band 5—Vegetation Red Edge</i>	0.705	20	15
<i>Band 6—Vegetation Red Edge</i>	0.740	20	15
<i>Band 7—Vegetation Red Edge</i>	0.783	20	20
<i>Band 8—NIR</i>	0.842	10	115
<i>Band 8A—Narrow NIR</i>	0.865	20	20
<i>Band 9—Water Vapour</i>	0.945	60	20
<i>Band 10—SWIR—Cirrus</i>	1.380	60	30
<i>Band 11—SWIR</i>	1.610	20	90
<i>Band 12—SWIR 20 180</i>	2.190	20	180

### 3.2 Regions of Interest (ROIs)

In this study, we focused on mapping secondary forest cover using a simple classification scheme. All the training data for the assigned land cover classes were identified by digital land cover map for 2013, high spatial resolution Spot 5 imagery for 2014 and high-resolution imagery from Google Earth. These images were converted to raster and opened with ENVI 5.1 software for algorithm training and validation of land cover classification. In the center of the individual land cover polygon, the ROI polygons were generated and dispersed as broadly as possible in the study area. All these geo-linked ROIs were saved in ENVI 5.1 format with the land cover map and Spot 5 images. The samples of training were split into five primary categories of land cover: water bodies, urban area, primary forest, secondary forest, and others.

**FIGURE 2. A SAMPLE OF SENTINEL-2A MSI'S TRUE COLOR COMPOSITE**

We used a total of 2168, taking into account the picture information, phenology and ROI size, including 1294 pixels Water Bodies ROIs, 1019 pixels Urban Area ROIs, 2973 pixels Primary Forest ROIs, 1495 pixels Secondary Forest ROIs, and 1622 pixels Others ROIs were included. To evaluate the efficiency of classification with a confusion matrix of different sample sizes, samples of different dimensions were chosen randomly by separating training from this ROI pool: 518 pixels Water Bodies ROIs, 408 pixels Urban Area ROIs, 1189 pixels Primary Forest ROIs, 598 pixels Secondary Forest ROIs, and 649 pixels Others ROIs were included. SVM, ANN and SAM classification techniques used the same randomly chosen training samples.

### 3.3 Spectral Separability Assessments

For purpose the spectral separability amongst land cover types, the M-statistic (Campbell & Wynne, 2011; Richards & Richards, 1999) with Jeffries–Matusita (J–M) distance method (Richards & Richards, 1999) were applied. The M-statistic defines class separability by mean and standard deviation values among two Landsat 8 sensor bands from two taster category distributions. M-statistics used in this research are provided as

$$M = (\mu_1 - \mu_2) / (\sigma_1 + \sigma_2)$$

where the mean reflectance value of land cover class 1 is  $\mu_1$ , the mean reflectance value of land cover class 2 is  $\mu_2$ ,  $\sigma_1$  is the standard deviation value of land cover class 1 and  $\sigma_2$  is the standard deviation value of land cover class 2. The value of  $M < 1$  shows that classes differ considerably and the capacity to separate areas is poor. At the other side, the value of  $M > 1$  shows that the means of the histogram are well separated and it is comparatively simple to discriminate among regions. M statistics of each pair of land cover categories were contrasted for six Landsat 8 spectral bands. The calculation of J–M is premised on distance from Bhattacharya. It enables to show how statistically distinct a chosen spectral class pair is. J–M distance is provided for two classes a and b as

$$JM_{ab} = \sqrt{2(1 - \exp(-\alpha))}$$

$$\alpha = \frac{1}{8}(\mu_a - \mu_b)^T \left(\frac{C_a + C_b}{2}\right)^{-1}(\mu_a - \mu_b) + \frac{1}{2} \ln \left[ \frac{\frac{1}{2}|C_a + C_b|}{\sqrt{|C_a||C_b|}} \right]$$

where  $\mu_a$  and  $\mu_b$  are the mean values for classes a and b,  $C_a$  and  $C_b$  are the covariance matrices for classes a and b, and T denotes the transpose of a vector. J–M range is an index of 0.0 to 2.0. Its  $> 1.7$  values show the classes are very well segregated. A distance J–M  $< 1.0$  shows bad separability between class pairs (Kumar et al., 2017).

Separability for all classes was investigated in ENVI software by calculating their spectral separability. Table 2 presents the outcomes of all feasible combinations to separate land cover classes. For Primary Forest, the overall pattern of JM values is quite comparable, and Secondary Forest classes with the separability values 1.7 show a good separation between these classes. (48). Whereas other classes are Primary Forest, Secondary Forest, and Urban Area classes, there is a significant distinction in value greater than 1.7 in the separability values among land classes that is moderate separation. According to (48) it is recognized. There are no pairs of land cover class that have A J–M range value  $< 1.0$  showing that different land cover classes are difficult to distinguish.

**TABLE 2. TRAINING SAMPLES SEPARABILITY VALUES BASED ON JEFFRIES-MATUSITA (J-M) INDEX FOR VARIOUS LAND COVER CLASSES**

<i>Land Cover Class</i>	<i>Water Bodies</i>	<i>Urban Area</i>	<i>Primary Forest</i>	<i>Secondary Forest</i>	<i>Others</i>
<i>Water Bodies</i>		<b>1.99</b>	<b>2</b>	<b>2</b>	<b>1.99</b>
<i>Urban Area</i>			<b>1.99</b>	<b>1.99</b>	<b>1.88</b>
<i>Primary Forest</i>				<b>1.73</b>	<b>1.83</b>
<i>Secondary Forest</i>					<b>1.78</b>
<i>Others</i>					

### 3.4 Mapping Algorithms

Figure 3 displays the workflow for secondary forest mapping. There have been multiple classification techniques and their accuracy has been evaluated. The algorithms for SVM, ANN and SAM were introduced and the outcomes were contrasted and efficiency was also checked for these techniques with distinct parameters.

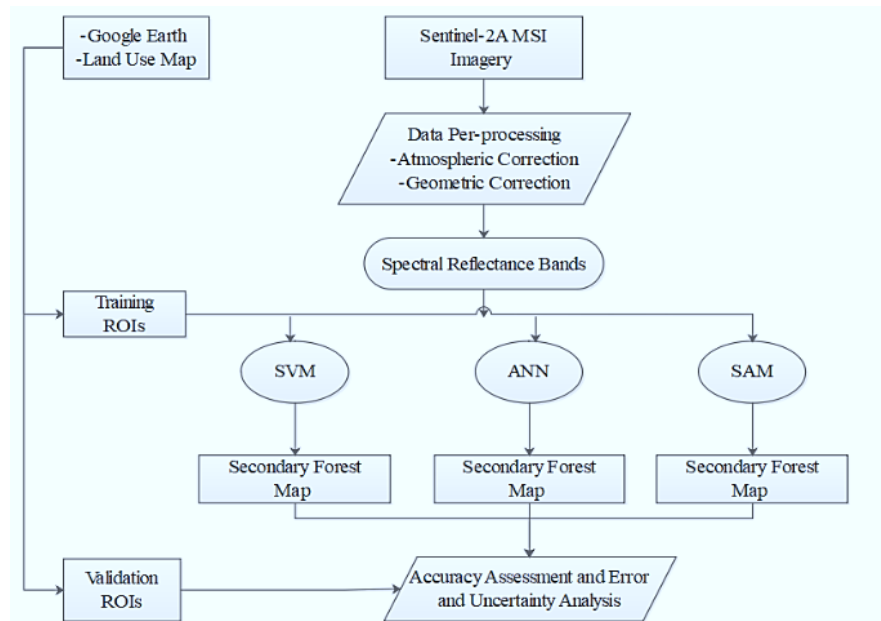


**FIGURE 3. THE WORKFLOW FOR MAPPING SECONDARY FOREST BASED ON SENTINEL-2 MSI 10-M IMAGERY**

#### a) SVM Classifier

SVM classifier is a non-parametric classifier of statistical learning without any assumptions about the fundamental distribution of information. It offers in terms of the generalization error to achieve the ideal separation hyper-plane for a training data set. A comprehensive SVM algorithm description can be discovered in the (49). We have chosen carefully kernel features to obtain excellent classification outcomes. Kernel features that match the ideal hyper plane separation in the high-dimensional space used in ENVI v.5.1 involve four kinds: linear, polynomial, sigmoid, and radial basis function (RBF). Many studies (50-55) (56, 57) compared of kernel function and setting parameters, and in most cases RBF is considered to work well. The RBF, which is normally a sensible option for mapping land cover (56-58), because of, first, the RBF kernel mapped samples non-linearly into a higher dimensional space so that the RBF was able to manage the situation when the relationship among class types and qualities was not linear. Second, the RBF kernel had fewer computing difficulties. We also attempted two more kernel features in this research: linear and polynomial, besides RBF. Considering the significance of kernel parameters optimization (55-57), for every kernel function, a variety of values were tested. For the polynomial and RBF kernels, the kernel radius ( $\gamma$ ) value was higher than 0, ranging from 0.1 to 10, whereas the regularization parameter (C) varied from 1 to 100. As suggested in the ENVI User Manual, other parameters such as the number of pyramid levels to be used and the classification probability threshold value were set (59). The precision of the classification and the Kappa coefficient were evaluated. With the RBF kernel function, the largest accuracies were obtained and the penalty value parameters C and the kernel parameter  $\gamma$  were set at 120 and 0.15, respectively. In relation, training datasets with various sizes of training samples (20, 50, 100, 200, 300, 400, 500 pixels per type) were investigated and then used to develop the SVM models to explore the impact of sample volume.

#### b) ANN Classifier

ANN is a human brain-inspired mathematical algorithm (60, 61), It is part of artificial intelligence methods, widely used in image analysis by computer instruments. According to (62, 63) An ANN is a parallel processing dispersed processor consisting of easy processing units with a natural propensity to store and make accessible experiential information. A typical ANN includes a big amount of easy processing units, known as nodes, connected by weighted links according to a specific architecture. (64). The simple ANN model comprises an input layer, a hidden layer, and a layer of output (Figure 4). Learning takes place by changing the node weights to reduce the distinction between the activation of the output node and the output. One can pick the number of hidden layers to use and choose among a feature of logistics or hyperbolic activation. A variety of parameters need to be set for the release of ANN. These include training rate, the training

threshold input, the training speed, the exit criteria field of RMS training and the number of concealed layers of using. The training speed defines the extent to which the weights are adjusted. A greater rate will accelerate the training and also increase the risk of the training consequence being oscillated or non-convergent. The input to the training limit determines the magnitude of the inner weight input to the activation level of the node and is used to adjust the modifications to the inner weight of a node. The training algorithm corrects the weights among nodes interactively and the node thresholds dynamically to reduce the mistake between the output layer and the required reaction. The training momentum is used to describe the training rate stage and its impact is to promote changes in weight in the present direction. A value greater than zero commonly enables a higher training rate to be set without oscillations. The entry criteria domain of the RMS training describes the error value of the RMS at which the training should stop. The number of hidden layers describes whether or not various input regions with a single hyperplane will be linearly separable. With no hidden layers (0 value), the various input areas are described as linearly separable with a single hyperplane, whereas if a greater value is used, non-linear classifications are conducted. Most of the ANN processors used in remote sensing are relying on a single hidden layer, but certain authors used two hidden layers in land cover classification networks. (see review by (60)). Reference (60) Already report that for most issues a single hidden layer should be adequate, particularly for classification assignments, since a multilayer perception with one layer can approximate any continuous function. Detailed illustrations of the concepts of the ANN parameters are offered with reference to their concepts, workflows and learning algorithms and their potential and constraints as can see in (60, 62, 63, 65). In the current research, using a logistic activation function in ENVI version 5.1 the ANN classifier used is a layered feed-forward model. The layers of the network are an input layer, an output layer, and one or more hidden layers. For supervised learning, it utilizes conventional backpropagation. The root mean square error (RMSE) between the real output of a multilayer feed-forward ANN and the required output was minimized by an iteration gradient algorithm of backpropagation.

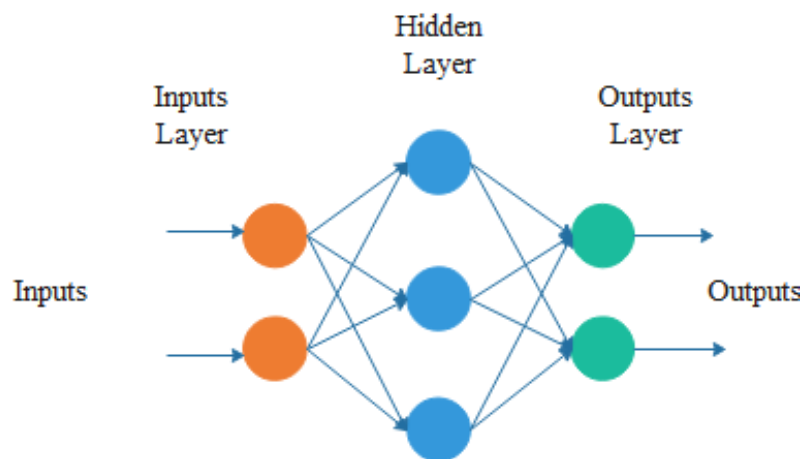


**FIGURE 4 REPRESENTATION OF THE OVERALL FRAMEWORK OF AN ANN, HERE WITH ONE HIDDEN LAYER (ADOPTED FROM(65))**

Once the RMSE achieved the optimum level, the iteration system was halted. A training limit value of 0.9, a training rate of 0.2, a training momentum of 0.9 and a training RMS exit criterion of 0.1 have been used in the current research. The number of iterations for training was set at 1,000 and one layer hidden was used. Various sizes of training samples (20, 50, 100, 200, 300, 400, 500 pixels for each variety) were used to assess the effect of training sample size on ANN.

### c) SAM Classifier

SAM is a spectral classifier capable of determining the spectral similarity between the image spectrum and the reference spectrum by measuring the angle among the spectra and treating them as vectors in a dimensionally equal space to the number of bands used each time (66, 67). Two source laboratory and field observations can be obtained from reference spectra for the application of the SAM method or can be extracted straight from the satellite imagery. In a multispectral n-dimensional space, a pixel vector has both magnitude (length) and angle calculated with respect to the axes defining the space's coordinate system (68). In cases of the form of the spectral pattern, the spectral similarity can also be evaluated utilizing angular distances (58) (69). SAM does not involve that the data be disseminated normally; they are not sensitive

to data variability and the size of the training data set (55, 70). In SAM, only angular data is used to define spectra of pixels, since the method is based on the premise that an observed reflectance spectrum is a vector in a multidimensional space where the number of dimensions is equal to the number of spectral bands. Small angles between the two spectrums show elevated similarity and elevated angles indicate low resemblance, whereas the given peak angle threshold pixels with an angle bigger than the tolerance rate are not categorized (59). The threshold value mainly expresses the highest appropriate angle of separation between the end-member spectrum vector and the pixel vector in the number of dimensional space bands (once more, here the Sentinel-2 MSI's four reflective bands) see Table 3. Pixels are not categorized with values greater than this threshold value. In the current study, SAM was introduced as the maximum threshold value for all classes in the ENVI v 5.1 image processing environment using a single value of 0.3 radians.

**TABLE 3. RESULTS OBTAINED IN SEPARATE SPECTRAL ANGLE EXPERIMENTS WITH MAXIMUM THRESHOLD VALUES FOR SAM**

<i>Classification method</i>	<i>Overall Accuracy %</i>	<i>Kappa Coefficient</i>
<i>SAM-1 (angle = 0.1)</i>	65.74	0.58
<i>SAM-2 (angle = 0.2)</i>	72.96	0.65
<i>SAM-3 (angle = 0.3)</i>	74.92	0.67
<i>SAM-4 (angle = 0.4)</i>	74.92	0.67
<i>SAM-5 (angle = 0.5)</i>	74.92	0.67

### 3.5 Accuracy Assessment

Secondary forest maps produced by the algorithms SVM, ANN and SAM validate as samples in individual locations from the entire research region via randomly chosen 3362 ROIs as seen in Section 4.2. In this research, error matrix statistics with validation samples were conducted, error metrics is a prevalent technique of evaluating classification precision (71, 72), from which the overall accuracy (OA), the accuracy of the producer (PA), the accuracy of the user (UA) and the kappa coefficient (Kc) were calculated as described:

$$OA = \frac{1}{N} \sum_{i=1}^r n_{ii},$$

$$PA = \frac{n_{ii}}{n_{icol}},$$

$$UA = \frac{n_{ii}}{n_{irow}},$$

$$K_c = N \sum_{i=1}^r n_{ii} - \sum_{i=1}^r \frac{n_{icol} n_{irow}}{N^2} - \sum_{i=1}^r n_{icol} n_{irow}$$

Where  $n_{ii}$  is the sample size of pixels classified accurately in the category;  $N$  is the total number of pixels in the confusion matrix;  $r$  is the number of rows, and  $n_{icol}$  and  $n_{irow}$  are the total column (source data) and row (expected classes) respectively. By dividing the sum of properly classified pixels to the total number of test pixels used for the classification, the OA can be evaluated. The UA is a commission error metric and indicates the likelihood that a class categorized on the map will truly represent that class on the ground. Likewise, PA is a measure of omission error and indicates the likelihood of proper classification of the real regions (68, 73, 74). The Kc was calculated to distinguish the real contract between the classes that actually took place on the ground vs. classified by opportunity classifiers (75). Kc analysis was also conducted to assess whether a certain classification was considerably better than a random classification and whether there were two significantly distinct classifications. A Kc value of 0 refers to a complete random classification, whereas a Kc value of 1 corresponds perfectly to the classification and reference data (71).

### 3.6 McNemar's Test

Using McNemar test, the importance of variations between these classification algorithms was calculated. It is beneficial to test the McNemar since it is parametric, very easy to comprehend and implement. It is also more accurate and delicate than the Kappa z-test (76-78). The test is premised on the normal standardized test as shown in Eq.2.

$$Z = \frac{f12 - f21}{\sqrt{f12 + f21}} \quad (2)$$

Where; f11, indicates the number of instances incorrectly categorized by both classifiers whereas f22 indicates the number of instances correctly categorized by both classifiers, although f12 and f21 are instances correctly categorized by one classifier but wrongly categorized by the other. (76-78). If the Z value is more than 1.96, a distinction in classification precision between the confusion matrices is statistically significant ( $p \leq 0.05$ ). (79, 80).

## IV. RESULTS

### 4.1 Secondary Forest Maps

Figure 5 showed secondary forest maps produced by the techniques of SVM, ANN, and SAM. According to ROI validation, the classification findings relying on Sentinel-2 MSI were very accurate. Table 4 shows the general accuracies and Kappa coefficients for the three techniques of classification. We just demonstrate the findings for scenarios using a larger sample size (518 pixels for water bodies, 408 pixels for urban region, 1189 pixels for primary forest, 598 pixels for secondary forest, and 649 pixels for other types of land cover). It is shown that the general accuracies and Kappa coefficients for SAM were 74 % and 0.67 respectively for a larger training sample size (more than 500 pixels per class), while the general accuracies and Kappa coefficients were above 90.78 % and 0.88 for the other classification techniques. The figure demonstrates that the outcome is excellent separability of the main and secondary forests.

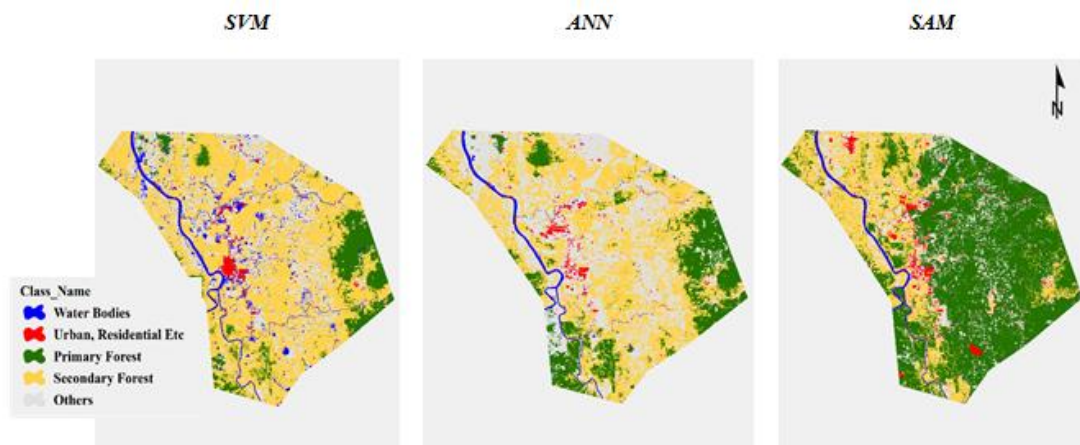


FIGURE 5. SECONDARY FOREST AREA MAPS FROM THREE CLASSIFICATION METHODS

TABLE 4. CONFUSION MATRIX FOR SVM, ANN AND SAM IN SECONDARY FOREST MAPPING ACCURACY.

Methods	Overall Accuracy %	Kappa Coefficient	Class	Ground Truth Samples (Pixels)					Total Classified Pixels	User Acc. (%)
				Water Bodies	Urban Area	Primary Forest	Secondary Forest	Other		
SVM	92.42	0.90	Water Bodies	518	89	0	0	184	791	100
			Urban Area	0	319	0	0	6	325	90.93
			Primary Forest	0	0	1050	24	0	1074	93.53
			Secondary Forest	0	0	139	573	66	778	84.84
			Other	0	0	0	1	393	394	92.66
			Total ground truth pixels	518	408	1189	598	649	3362	
			Prod. Acc. (%)	95.37	95.83	93.69	86.12	91.37		
ANN	90.78	0.88	Water Bodies	508	3	0	0	2	513	99.03
			Urban Area	5	389	0	0	40	434	89.63
			Primary Forest	0	0	1050	64	0	1114	94.25
			Secondary Forest	0	0	139	523	25	687	76.13
			Other	5	16	0	11	582	614	94.79
			Total ground truth pixels	518	408	1189	598	649	3362	
			Prod. Acc. (%)	98.07	95.34	88.31	87.46	89.68		
SAM	74.79	0.67	Water Bodies	427	0	0	0	0	427	100
			Urban Area	17	323	0	0	43	383	84.33
			Primary Forest	0	0	814	217	0	1031	78.95
			Secondary Forest	0	0	375	381	141	897	42.47
			Other	6	13	0	0	464	483	96.07
			Total ground truth pixels	450	336	1189	598	648	3221	
			Prod. Acc. (%)	94.89	96.13	68.46	63.71	71.6		

#### 4.2 Accuracy Assessment with Various Sizes of Training Samples and McNemar's Test

We calculated the overall accuracies and Kappa coefficients for various training sample sizes to evaluate the performance variation of the three classification methods with various training sample sizes, and the outcomes is shown in Figure 6. The output of SVM surpassed ANN and SAM for nearly all assigned training sample sizes, as per the general accuracies and Kappa coefficients. The general precision and Kappa coefficient of SVM were 92.42 % and 0.90 respectively for large training dimensions (i.e. no less than 500 pixels per class). The findings of SVM were almost identical to those of ANN (90.78 % for overall precision and 0.88 % for Kappa) and mildly superior to those of SAM (74.79 % for overall precision and 0.67 % for Kappa). The SVM and ANN techniques had greater overall accuracies and Kappa coefficients when the training sample size was lower, with superior overall accuracies 21% above SAM. Once training samples increased, the performance of accuracy enhanced quickly for the SAM technique. Whereas the increase in accuracy results was moderate for the SVM and ANN process. When the size of the training was sufficiently large (more than 500 pixels per class), ANN and SVM were equally precise and higher than the SAM technique. In Kappa coefficients, the same trends emerged as in the overall accuracies. It is clear that the size of the training sample had less effect on the classification of SVM and ANN than on SAM. The overall accuracies and coefficients of Kappa indicate that SVM outperformed the other two techniques of classification.

Table 5 demonstrates that the test value Z and P between SVM, ANN and SAM of the McNemar varied from 29 (significant) to -25.03 (negligible), based on the sample size of the practice. With tiny sample sizes that decreased with enhanced training sample size, SVM had no important benefit. The McNemar test for SVM and SAM produced Z values ranging from -16.80 to 24.03 in favor of SVM at 200 sample sizes of practice. Z values varied as per the sample size of the training sample for ANN and SAM; when the sample size of the training sample expanded, the Z value often improved. It should be observed that no training sample was required as a SAM technique, so the growing Z values further demonstrate that SVM / ANN's efficiency increased along with increased training size. SVM thus had a substantial benefit over ANN and SAM. Table 5 form it the McNemar's SVM, ANN, and SAM test. If the test value of the McNemar is higher than 1.96, the first technique offers a statistically significant enhancement in the outcomes of the classification. If the test value of the McNemar is less than -1.96, the former technique will have a statistically significantly lower output than the latter.

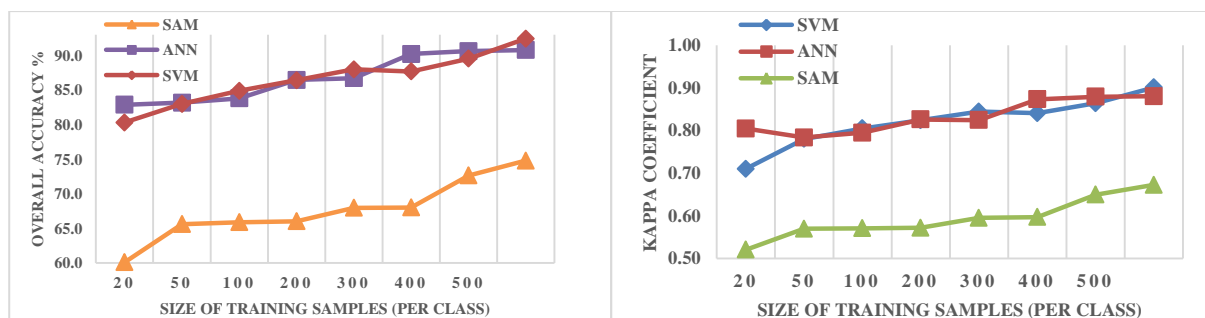


FIGURE 6. THE OA AND K-COEFFICIENTS OF CLASSIFICATION METHODS SVM, ANN AND SAM

TABLE 5 THE Z AND P VALUE OF MCNEMAR AMONG SVM, ANN AND SAM

Classification Method		Size of Training Samples (Per Class)						
		20 Pixels	50 Pixels	100 Pixels	200 Pixels	300 Pixels	400 Pixels	500 Pixels
SVM vs. ANN	z value	-25.03	-0.57	-3.13	-8.63	6.96	-7.63	-2.88
	p value	0.0001	0.637	0.002	0.0001	0.0001	0.0001	0.005
SVM vs. SAM	z value	-16.80	15.64	17.18	24.03	20.82	19.07	21.60
	p value	0.0001	0.0001	0.0001	0.0001	0.0001	0.0001	0.0001
ANN vs. SAM	z value	14.581	16.264	20.327	28.860	16.919	23.825	23.674
	p value	0.0001	0.0001	0.0001	0.0001	0.0001	0.0001	0.0001

## V. DISCUSSION

### 5.1 Source of Uncertainty and Errors

Numerous variables influence classification accuracy, like the technique of classification, source of information for remote sensing, and choice of samples for training. The 2018 Sentinel-2 MSI information was used in this research, but we selected training samples and validation samples based on Google Earth whose distant pictures were acquired in our research region in 2013–2017. Several land cover transfer may have happened throughout this time. Our result may have implemented some confusion or even error in the difference in image acquisition time. The region of the water could be underestimated. There's a lengthy river in the study region. The river width is small, typically less than 50 m, which in the Sentinel-2 MSI picture is more than one-pixel wide. Furthermore, the Sentinel-2 MSI picture that we used for this research was obtained during the dry season, meaning that river and maybe some channels had little water or even run dry. We can, therefore, be quite confident that the water samples we chose did not include the river region. The region of the measured secondary forest region is probable to be lower than the region in question. Primary forest region has been the primary target in this research. The secondary forest training samples were primarily from orchards of mature trees. Due to variations in spectral features among freshly planted secondary forest and mature secondary forest, many newly planted secondary forest area, usually encircled by grass, and could be ignored. For instance, the distinction between newly planted areas and mature secondary forest is around 4 in the Sentinel-2 MSI information (81). Research with comprehensive samples at various phases of development will be used in future research to evaluate spectral features and recognize secondary forests at various types and ages.

### 5.2 Potential Application of These Classification Methods

We need a decent consideration of the results of these techniques in order to make ideal use of the actual classification technique. In most cases, SVM exceeds the other two algorithms in classification accuracy. However, in order to select an appropriate algorithm, all the probable pros and cons particular to the scenario must be taken into consideration, not only in terms of precision as well as in terms of model parameters, speed, and ease of use. As mentioned above, the SVM technique must set and modify model parameters. Most definitely, weak parameters will produce poor outcomes. SVM loses to ANN and SAM when it comes to speed. (58). SVM classification will take a lot longer in the training phase and in the real information classification phase, especially for a big remote sensing dataset, creating SVM unfit for regional or global classification (58). No extra model parameters are required for ANN and SAM algorithms and they are less time-consuming. The SVM technique does not require time for training or prior statistical spectral analyzes, but requires the involvement of an expert, so its performance relies on the operator spectral skills and knowledge. The structure of the ANN varies with the size of the training data using ANN method. If this rule can be introduced widely to secondary forest mapping, the decision method also need no samples of practice and will be the fastest and simplest among the three techniques. Additional factors for selecting an algorithm should also include input information and the required result for a specified implementation. In coping with noisy data, SVM is not great. Pre-processing will, therefore, be very essential for microwave remote sensing information when using SVM to map the secondary forest cover. Furthermore, for automatic classification, the quality of training samples is of excellent concern. For SVM, the outcome of classification will be significantly impaired by a comparatively tiny amount of mislabeled training samples. Thus, while SVM requires fewer samples, it requires samples of high quality training. The ANN technique requires not only excellent quality but also excellent volume training samples. SVM is the ideal technique for sub-regional level classification given its speed and classification accuracy, whereas ANN is the superior algorithm for secondary forest cover classification at regional and global scales if a big amount of training samples are accessible. SAM is the second to none selection between these three techniques if no training samples are accessible. If the based ANN is appropriate for other areas, the ANN method will also require no training samples and in any scenario will be the most relevant method.

## VI. CONCLUSIONS

Global and regional forest request has led in comprehensive development and extension of the secondary forest region and also the transformation of land cover from natural tropical rainforests to cultivated agro-forests with related deforestation over a big region, especially in tropical areas. To monitor and evaluate the effects of these property, conversions must be mapped correctly and in a timely way on the environment, biodiversity, and carbon cycle, but also on

local economy. Sentinel-2 MSI information and three classification techniques were studied in this document to map secondary forest area in Kelantan test area, a secondary forest area hotspot area. Various training sample sizes (20, 50, 100, 200, 300, 400, 500 pixels for each type) and parameters were used to evaluate the efficiency of the three separate classification techniques.

The findings indicate that a map of the secondary forest area with a spatial resolution of 10 m can be achieved utilizing Sentinel-2 MSI information with general accuracies and Kappa coefficients above 92.42 % and 0.90 respectively for a larger sample size of training (i.e. more than 500 pixels per class). The lower the sample size of the practice, the greater the SVM's superiority. SVM was the most time-consuming technique, but, particularly when mapping a big region was involved. SAM, compares quicker with others. However, for a larger training sample size, it is less precise with lower general accuracies 17 % below SVM and 15 % below ANN. ANN was a compromise on speed and accuracy, but enough training data was required. Consideration is given to selecting an appropriate algorithm for secondary forest mapping, information size, accessible training data, scope of research region, and time necessity.

#### ACKNOWLEDGMENTS

Authors would like to thank Prof. Shattri B. Mansor, Director of Remote Sensing and GIS Research Center and Dr. Zailani Khuzaimah for financial assistance, suggestions, and guidelines. The authors also want to thank Universiti Putra Malaysia for its helpful, as well as expressing the thanks to both anonymous reviewers for their comments and suggestions.

#### REFERENCES

- [1] Gómez C, White JC, Wulder MAJJoP, Sensing R. Optical remotely sensed time series data for land cover classification: A review. 2016;116:55-72.
- [2] Immitzer M, Vuolo F, Atzberger CJRS. First experience with Sentinel-2 data for crop and tree species classifications in central Europe. 2016;8(3):166.
- [3] Szostak M, Hawryło P, Piela DJEJoRS. Using of Sentinel-2 images for automation of the forest succession detection. 2018;51(1):142-9.
- [4] Petropoulos GP, Vadrevu KP, Kalaitzidis CJGi. Spectral angle mapper and object-based classification combined with hyperspectral remote sensing imagery for obtaining land use/cover mapping in a Mediterranean region. 2013;28(2):114-29.
- [5] Griffiths P, Kuemmerle T, Baumann M, Radeloff VC, Abrudan IV, Lieskovsky J, et al. Forest disturbances, forest recovery, and changes in forest types across the Carpathian ecoregion from 1985 to 2010 based on Landsat image composites. 2014;151:72-88.
- [6] Wulder MA, White JC, Loveland TR, Woodcock CE, Belward AS, Cohen WB, et al. The global Landsat archive: Status, consolidation, and direction. 2016;185:271-83.
- [7] Azzari G, Lobell DJRSO. Landsat-based classification in the cloud: An opportunity for a paradigm shift in land cover monitoring. 2017;202:64-74.
- [8] Clerici N, Valbuena Calderón CA, Posada JMJoM. Fusion of Sentinel-1A and Sentinel-2A data for land cover mapping: a case study in the lower Magdalena region, Colombia. 2017;13(2):718-26.
- [9] Shen G, Sakai K, Hoshino YJAIR. High spatial resolution hyperspectral mapping for forest ecosystem at tree species level. 2010;19(3):71-8.
- [10] Kachmar M, Sánchez-Azofeifa GA, Rivard B, Kakubari YJMR, Development. Improved forest cover classification in an industrialized mountain area in Japan. 2005;25(4):349-56.
- [11] Singh AJJoRS. Spectral separability of tropical forest cover classes. 1987;8(7):971-9.

- [12] Yuan F, Sawaya KE, Loeffelholz BC, Bauer MEJRsoE. Land cover classification and change analysis of the Twin Cities (Minnesota) Metropolitan Area by multitemporal Landsat remote sensing. 2005;98(2-3):317-28.
- [13] Steining MJIJoRS. Tropical secondary forest regrowth in the Amazon: age, area and change estimation with Thematic Mapper data. 1996;17(1):9-27.
- [14] García M, Saatchi S, Ustin S, Balzter HJIJoaoe, geoinformation. Modelling forest canopy height by integrating airborne LiDAR samples with satellite Radar and multispectral imagery. 2018;66:159-73.
- [15] Kuntz S, Siegert FJIJoRS. Monitoring of deforestation and land use in Indonesia with multitemporal ERS data. 1999;20(14):2835-53.
- [16] Jin H, Mountrakis G, Stehman SVJIJoP, Sensing R. Assessing integration of intensity, polarimetric scattering, interferometric coherence and spatial texture metrics in PALSAR-derived land cover classification. 2014;98:70-84.
- [17] Saatchi S, Agosti D, Alger K, Delabie J, Musinsky JJCB. Examining fragmentation and loss of primary forest in the southern Bahian Atlantic forest of Brazil with radar imagery. 2001;15(4):867-75.
- [18] Simard M, Grandi GD, Saatchi S, Mayaux PJIJoRS. Mapping tropical coastal vegetation using JERS-1 and ERS-1 radar data with a decision tree classifier. 2002;23(7):1461-74.
- [19] Podest E, Saatchi SJIJoRS. Application of multiscale texture in classifying JERS-1 radar data over tropical vegetation. 2002;23(7):1487-506.
- [20] Hoekman DHJIJoRS. Radar backscattering of forest stands. 1985;6(2):325-43.
- [21] Luckman AJIItog, sensing r. The effects of topography on mechanisms of radar backscatter from coniferous forest and upland pasture. 1998;36(5):1830-4.
- [22] Bayer T, Winter R, Schreier GJIToG, Sensing R. Terrain influences in SAR backscatter and attempts to their correction. 1991;29(3):451-62.
- [23] Goyal S, Seyfried M, O'Neill PJIJoRS. Effect of digital elevation model resolution on topographic correction of airborne SAR. 1998;19(16):3075-96.
- [24] Malenovsky Z, Rott H, Cihlar J, Schaepman ME, García-Santos G, Fernandes R, et al. Sentinels for science: Potential of Sentinel-1,-2, and-3 missions for scientific observations of ocean, cryosphere, and land. 2012;120:91-101.
- [25] Belward AS, Skøien JOJIJoP, Sensing R. Who launched what, when and why; trends in global land-cover observation capacity from civilian earth observation satellites. 2015;103:115-28.
- [26] Augustin H, Sudmanns M, Tiede D, Baraldi AJPotA. A semantic Earth observation data cube for monitoring environmental changes during the Syrian conflict. 2018:214-27.
- [27] Rogan J, Chen DJPip. Remote sensing technology for mapping and monitoring land-cover and land-use change. 2004;61(4):301-25.
- [28] Lu D, Batistella M, Li G, Moran E, Hetrick S, Freitas CdC, et al. Land use/cover classification in the Brazilian Amazon using satellite images. 2012;47(9):1185-208.
- [29] Li G, Lu D, Moran E, Hetrick SJIjors. Land-cover classification in a moist tropical region of Brazil with Landsat Thematic Mapper imagery. 2011;32(23):8207-30.
- [30] Rodriguez-Galiano VF, Ghimire B, Rogan J, Chica-Olmo M, Rigol-Sanchez JPJIJoP, Sensing R. An assessment of the effectiveness of a random forest classifier for land-cover classification. 2012;67:93-104.
- [31] Friedl MA, McIver DK, Hodges JC, Zhang XY, Muchoney D, Strahler AH, et al. Global land cover mapping from MODIS: algorithms and early results. 2002;83(1-2):287-302.

- [32] Blackard JA, Dean DJJC, agriculture ei. Comparative accuracies of artificial neural networks and discriminant analysis in predicting forest cover types from cartographic variables. 1999;24(3):131-51.
- [33] Kuching SJJCS. The performance of maximum likelihood, spectral angle mapper, neural network and decision tree classifiers in hyperspectral image analysis. 2007;3(6):419-23.
- [34] Dixon B, Candade NJJoRS. Multispectral landuse classification using neural networks and support vector machines: one or the other, or both? 2008;29(4):1185-206.
- [35] Trebar M, Steele NJC, Agriculture Ei. Application of distributed SVM architectures in classifying forest data cover types. 2008;63(2):119-30.
- [36] Mondal A, Kundu S, Chandniha SK, Shukla R, Mishra PJIJoRS, GIS. Comparison of support vector machine and maximum likelihood classification technique using satellite imagery. 2012;1(2):116-23.
- [37] Nitze I, Schulthess U, Asche HJPottG. Comparison of machine learning algorithms random forest, artificial neural network and support vector machine to maximum likelihood for supervised crop type classification. 2012:7-9.
- [38] Pal M, Foody GMJIJoStiAEO, Sensing R. Evaluation of SVM, RVM and SMLR for accurate image classification with limited ground data. 2012;5(5):1344-55.
- [39] Lu D, Weng Q, Moran E, Li G, Hetrick S. Remote sensing image classification: CRC Press/Taylor and Francis: Boca Raton, FL, USA; 2011.
- [40] Gašparović M, Jogun TJIJoRS. The effect of fusing Sentinel-2 bands on land-cover classification. 2018;39(3):822-41.
- [41] Morfitt R, Barsi J, Levy R, Markham B, Micijevic E, Ong L, et al. Landsat-8 Operational Land Imager (OLI) radiometric performance on-orbit. 2015;7(2):2208-37.
- [42] Northrop A, Team LJUKTVUL. IDEAS–LANDSAT Products Description Document. 2015.
- [43] Coppin P, Jonckheere I, Nackaerts K, Muys B, Lambin EJJjors. Review Article Digital change detection methods in ecosystem monitoring: a review. 2004;25(9):1565-96.
- [44] Mas J-FJJjors. Monitoring land-cover changes: a comparison of change detection techniques. 1999;20(1):139-52.
- [45] Huang C, Goward SN, Schleeweis K, Thomas N, Masek JG, Zhu ZJRsoE. Dynamics of national forests assessed using the Landsat record: Case studies in eastern United States. 2009;113(7):1430-42.
- [46] Yuan D, Elvidge CJRsoe. NALC land cover change detection pilot study: Washington DC area experiments. 1998;66(2):166-78.
- [47] Kennedy RE, Cohen WB, Schroeder TAJRSOE. Trajectory-based change detection for automated characterization of forest disturbance dynamics. 2007;110(3):370-86.
- [48] Kumar P, Prasad R, Choudhary A, Mishra VN, Gupta DK, Srivastava PKJGi. A statistical significance of differences in classification accuracy of crop types using different classification algorithms. 2017;32(2):206-24.
- [49] Burges CJDm, discovery k. A tutorial on support vector machines for pattern recognition. 1998;2(2):121-67.
- [50] Foody GM, Mathur AJITog, sensing r. A relative evaluation of multiclass image classification by support vector machines. 2004;42(6):1335-43.
- [51] Kavzoglu T, Colkesen IJIJoAEO, Geoinformation. A kernel functions analysis for support vector machines for land cover classification. 2009;11(5):352-9.
- [52] Pal MJIJoRS. Support vector machine-based feature selection for land cover classification: a case study with DAIS hyperspectral data. 2006;27(14):2877-94.

- [53] Petropoulos GP, Kalaitzidis C, Vadrevu KPJC, Geosciences. Support vector machines and object-based classification for obtaining land-use/cover cartography from Hyperion hyperspectral imagery. 2012;41:99-107.
- [54] Yang XJPE, Sensing R. Parameterizing support vector machines for land cover classification. 2011;77(1):27-37.
- [55] Petropoulos GP, Vadrevu KP, Xanthopoulos G, Karantounias G, Scholze MJS. A comparison of spectral angle mapper and artificial neural network classifiers combined with Landsat TM imagery analysis for obtaining burnt area mapping. 2010;10(3):1967-85.
- [56] Jia K, Wei X, Gu X, Yao Y, Xie X, Li BJGI. Land cover classification using Landsat 8 operational land imager data in Beijing, China. 2014;29(8):941-51.
- [57] Kavzoglu T, Colkesen IJjors. An assessment of the effectiveness of a rotation forest ensemble for land-use and land-cover mapping. 2013;34(12):4224-41.
- [58] Kumar P, Gupta DK, Mishra VN, Prasad RJIJoRS. Comparison of support vector machine, artificial neural network, and spectral angle mapper algorithms for crop classification using LISS IV data. 2015;36(6):1604-17.
- [59] Guide EUsJIVIS. ENVI on-line software user's manual. 2008.
- [60] Mas JF, Flores JJIJoRS. The application of artificial neural networks to the analysis of remotely sensed data. 2008;29(3):617-63.
- [61] Civco DLJIJoGIS. Artificial neural networks for land-cover classification and mapping. 1993;7(2):173-86.
- [62] Atkinson PM, Tatnall ARJIJors. Introduction neural networks in remote sensing. 1997;18(4):699-709.
- [63] Miller DM, Kaminsky EJ, Rana SJC, Geosciences. Neural network classification of remote-sensing data. 1995;21(3):377-86.
- [64] Srivastava PK, Han D, Rico-Ramirez MA, Bray M, Islam TJAiSR. Selection of classification techniques for land use/land cover change investigation. 2012;50(9):1250-65.
- [65] Kanellopoulos I, Wilkinson GGJIJoRS. Strategies and best practice for neural network image classification. 1997;18(4):711-25.
- [66] Kruse FA, Lefkoff A, Boardman J, Heidebrecht K, Shapiro A, Barloon P, et al. The spectral image processing system (SIPS)—interactive visualization and analysis of imaging spectrometer data. 1993;44(2-3):145-63.
- [67] Hunter E, Power CJIJoRS. An assessment of two classification methods for mapping Thames Estuary intertidal habitats using CASI data. 2002;23(15):2989-3008.
- [68] Lillesand T, Kiefer RW, Chipman J. Remote sensing and image interpretation: John Wiley & Sons; 2014.
- [69] Sohn Y, Morán E, Gurri FJPE, Sensing R. Deforestation in North-Central Yucatan 1985-1995): Mapping secondary succession of forest and agricultural land use in Sotuta using the cosine of the angle concept. 1999;65(8):947-58.
- [70] Sohn Y, Rebello NSJPe, sensing r. Supervised and unsupervised spectral angle classifiers. 2002;68(12):1271-82.
- [71] Congalton RG, Green KJLP-LBR, FL, USA. Assessing the accuracy of remotely sensed data: principles and applications. 1999.
- [72] Congalton RG, Green K. Assessing the accuracy of remotely sensed data: principles and practices: CRC press; 2008.
- [73] Foody GMJRsoe. Status of land cover classification accuracy assessment. 2002;80(1):185-201.
- [74] Olofsson P, Foody GM, Herold M, Stehman SV, Woodcock CE, Wulder MAJRSoE. Good practices for estimating area and assessing accuracy of land change. 2014;148:42-57.
- [75] Cohen JJE, measurement p. A coefficient of agreement for nominal scales. 1960;20(1):37-46.
- [76] Foody GMJPIPG. Map comparison in GIS. 2007;31(4):439-45.

- [77] Foody GMJPE, Sensing R. Thematic map comparison. 2004;70(5):627-33.
- [78] de Leeuw J, Jia H, Yang L, Liu X, Schmidt K, Skidmore AJJoRS. Comparing accuracy assessments to infer superiority of image classification methods. 2006;27(1):223-32.
- [79] Manandhar R, Odeh IO, Ancev TJRS. Improving the accuracy of land use and land cover classification of Landsat data using post-classification enhancement. 2009;1(3):330-44.
- [80] Congalton RG, Oderwald RG, Mead RAJPe, sensing r. Assessing Landsat classification accuracy using discrete multivariate analysis statistical techniques. 1983;49(12):1671-8.
- [81] Mandanici E, Bitelli GJRS. Preliminary comparison of Sentinel-2 and Landsat 8 Imagery for a combined use. 2016;8(12):1014.